Inorg. Chem. **2004**, *43*, 969–977

Problem of a Wide Variety of Products in the $Cu(hfac)_2$–Nitroxide System

Sergei Fokin, Victor Ovcharenko,* Galina Romanenko, and Vladimir Ikorskii

International Tomography Center, Russian Academy of Sciences, Institutskaya 3a, 630090 Novosibirsk, Russia

Received August 13, 2003

The stereochemically flexible $Cu(hfac)_2$ metal–ligand system when combined with polyfunctional nitroxides leads to a variety of solids with varying structure and composition. While investigating the products of $Cu(hfac)_2$ interaction with spin-labeled pyrazole 4,4,5,5-tetramethyl-2-(1-methyl-1*H*-pyrazol-4-yl)-imidazoline-3-oxide-1-oxyl, we have isolated a family of (12) heterospin compounds differing in structure and composition in the solid state. In synthetic systems, these compounds often cocrystallize and must be separated mechanically. It is also shown that minor variation of the structure of the solid heterospin complex can substantially change the magnetic properties of compounds.

Introduction

$Cu(hfac)_2$ is widely used in the synthesis of molecular magnets (hfac = hexafluoroacetylacetonate).[1−3] On the one hand, this is a strong acceptor readily forming complexes with a coordinated nitroxyl group. On the other hand, its interactions with nitroxides yield heterospin systems whose magnetic properties are convenient for subsequent theoretical analysis. In recent years, syntheses of heterospin systems have employed increasingly complicated polyfunctional derivatives of stable nitroxides, which favor the formation of highly dimensional structures and heterospin exchange clusters of varying structure.[4−6] By modification of the paramagnetic ligand molecule, one can change the structure and the magnetic behavior of the exchange cluster, which opens up favorable opportunities for sequential definition of magnetostructural correlations.

At present, there are many known heterospin complexes of $Cu(hfac)_2$ with nitroxides, varying in structure and composition.[4−25] Some of them possess nontrivial magnetic properties.[20−25] These include a complex with spin-labeled pyrazole $Cu(hfac)_2L$ (denoted below as complex **1**), for which we have previously found a thermally induced

* To whom correspondence should be addressed. Phone: +7-3832-33-1222. Fax: +7-3832-33-1399. E-mail: ovchar@tomo.nsc.ru.

(1) Caneschi, A.; Gatteschi, D.; Rey, P. *Prog. Inorg. Chem.* **1993**, *39*, 331.
(2) Kahn, O. *Molecular Magnetism*; VCH: NewYork, 1993.
(3) Ovcharenko, V. I.; Sagdeev, R. Z. *Russ. Chem. Rev.* **1999**, *68*, 345 (Engl. Transl.).
(4) Burdukov, A. B.; Gushin, D. A.; Pervukhina, N. V.; Ikorskii, V. N.; Shvedenkov, Yu. G.; Reznikov, V. A.; Ovcharenko, V. I. *Cryst. Eng.* **1999**, *2*, 265.
(5) Griesar, K.; Haase, W.; Svoboda, I.; Fuess, H. *Inorg. Chim. Acta* **1999**, *287*, 181.
(6) Caneschi, A.; Ferraro, F.; Gatteschi, D.; Rey, P.; Sessoli, R. *Inorg. Chem.* **1991**, *30*, 3162.
(7) Burdukov, A. B.; Ovcharenko, V. I.; Pervukhina, N. V.; Ikorskii, V. N.; Kiriluk, I. A.; Grigoriev, I. A. *Polyhedron* **1995**, *14*, 501.
(8) Jiang, Z.-H.; Yi, Q.; Liao, D.-Z.; Huan, Z.-W.; Yan, S.-P.; Wang, G.-L.; Yao, X.-K.; Wang, R.-J. *Transition Met. Chem.* **1995**, *20*, 136.
(9) Caneschi, A.; David, L.; Ferraro, F.; Gatteschi, D.; Fabretti, A. C. *Inorg. Chim. Acta* **1994**, *217*, 7.
(10) Burdukov, A. B.; Ovcharenko, V. I.; Pervukhina, N. V.; Ikorskii, V. N. *Polyhedron* **1993**, *12*, 1705.
(11) Ishimaru, Y.; Kitano, M.; Kumada, H.; Koga, N.; Iwamura, H. *Inorg. Chem.* **1998**, *37*, 2273.
(12) Gatteschi, D.; Laugier, J.; Rey, P.; Zanchini, C. *Inorg. Chem.* **1987**, *26*, 938.
(13) Caneschi, A.; Gatteschi, D.; Laugier, J.; Rey, P. *J. Am. Chem. Soc.* **1987**, *109*, 2191.
(14) Burdukov, A. B.; Ovcharenko, V. I.; Pervukhina, N. V.; Ikorskii, V. N. *Zh. Neorg. Khem. (Russ.)* (*Russ. J. Inorg. Chem.*) **1993**, *38*, 496.
(15) Pervukhina, N. V.; Podberezskaya, N. V. *Zh. Strukt. Khim. (Russ.)* (*Russ. J. Struct. Chem.*) **1994**, *35*−*3*, 141.
(16) Mori, H.; Nagao, O.; Kozaki, M.; Shiomi, D.; Sato, K.; Takui, T.; Okada, K. *Polyhedron* **2001**, *20*, 1663.
(17) Burdukov, A. B.; Ovcharenko, V. I.; Ikorskii, V. N.; Pervukhina, N. V.; Podberezskaya, N. V.; Grigor'ev, I. A.; Larionov, S. V.; Volodarsky, L. B. *Inorg. Chem.* **1991**, *30*, 972.
(18) Caneschi, A.; Chiesi, P.; David, L.; Ferraro, F.; Gatteschi, D.; Sessoli, R. *Inorg. Chem.* **1993**, *32*, 1445.
(19) Zhang, D.; Liu, W.; Xu, W.; Jin, X.; Zhu, D. *Inorg. Chim. Acta* **2001**, *318*, 84.
(20) Luneau, D.; Rey, P.; Laugier, J.; Fries, P.; Caneschi, A.; Gatteschi, D.; Sessoli, R. *J. Am. Chem. Soc.* **1991**, *113*, 1245.
(21) Lanfranc de Panthou, F.; Belorizky, E.; Calemczuk, R.; Luneau, D.; Marcenat, C.; Ressouche, E.; Turek, P.; Rey, P. *J. Am. Chem. Soc.* **1995**, *117*, 11247.
(22) Lanfranc de Panthou, F.; Luneau, D.; Musin, R.; Ohrstrom, L.; Grand, A.; Turek, P.; Rey, P. *Inorg. Chem.* **1996**, *35*, 3484.
(23) Iwahory, F.; Inoue, K.; Iwamura, H. *Mol. Cryst. Liq. Cryst.* **1999**, *334*, 533.
(24) Ovcharenko, V. I.; Fokin, S. V.; Romanenko, G. V.; Ikorskii, V. N.; Tretyakov, E. V.; Vasilevsky, S. F. *J. Struct. Chem.* **2002**, *43*, 153.

10.1021/ic034964d CCC: $27.50
Published on Web 01/15/2004

Chart 1

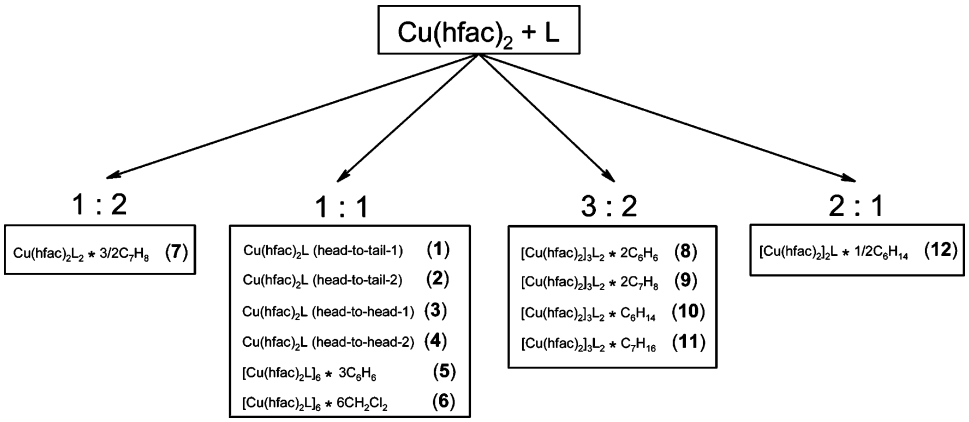

magnetic effect similar to spin crossover (Figure 4).[24] However, **1** can only be obtained under definite synthetic conditions. Variation of conditions can lead to solids with different structures and compositions. The stereochemical nonrigidity of $Cu(hfac)_2$ also favors the formation of products in increased numbers. Previously, formation of two polymorphic modifications in the reaction of $Cu(hfac)_2$ with the same nitroxide has been reported.[12,18−20] When investigating the products of $Cu(hfac)_2$ interaction with spin-labeled pyrazole L, to our surprise we isolated *twelve* solids differing in structure and composition. They may be classified into four groups according to their $Cu(hfac)_2$/L ratio: see Chart 1.

Five of these (**1**−**5**) are actually polymorphs (the fifth modification obtained from **5** or **6** by solvent removal). For all heterospin complexes **1**−**12**, we determined their crystal and molecular structures. Magnetic studies did not reveal any magnetic anomalies deserving special attention except in **1** and **3**. We have also found that even seemingly insignificant changes in the structure of the solid can substantially change the magnetic properties of the compound. Therefore, in this paper, we indicate that the stereochemically nonrigid matrix of $Cu(hfac)_2$, widely employed in heterospin system design, shows very different behaviors with polyfunctional nitroxides, leading to products with different structures and compositions.

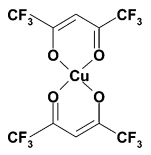

$Cu(hfac)_2$

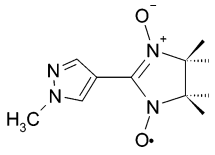

L

Experimental Section

Synthesis of the Compounds. 4,4,5,5-Tetramethyl-2-(1-methyl-1*H*-pyrazol-4-yl)-imidazoline-3-oxide-1-oxyl (L) was synthesized according to a known procedure.[24]

$Cu(hfac)_2$L (1, or "Head-to-Tail"-1). A mixture of $Cu(hfac)_2$ (0.1007 g, 0.21 mmol) and L (0.0500 g, 0.21 mmol) was dissolved with heating to 50 °C in hexane (20 mL). The resulting dark brown solution was quickly filtered and cooled to room temperature. After a few minutes, prismatic crystals formed; they were filtered off, washed with cold hexane, and dried in air. Yield 65%. The complex is soluble in most organic solvents. It gradually decomposes when stored in solution for a day or more. Recrystallization from toluene yielded very large dark blue hexagonal prisms. Gradual concentration of an acetone/hexane or acetone/heptane solution by solvent removal with a flow of air gave aggregates of dark blue needle crystals **1**. The composition and magnetic properties of **1** were the same in all synthetic procedures. Calculated for $C_{21}H_{19}N_4O_6F_{12}Cu$, %: C, 35.3; H, 2.7; N, 7.8; F, 31.9. Found, %: C, 35.1; H, 2.8; N, 7.5; F, 32.0.

$Cu(hfac)_2$L (2, or "Head-to-Tail"-2). A mixture of $Cu(hfac)_2$ (0.1000 g, 0.21 mmol) and L (0.0331 g, 0.14 mmol) was dissolved with stirring and heating to 50 °C in a mixture of heptane (20 mL) and CH_2Cl_2 (2 mL). The resulting dark brown solution was quickly filtered and cooled to room temperature. A few minutes later, fine dark blue crystals of two types formed, which differed in habit; they were filtered off, washed with cold heptane, and dried in air. The bulk of the product was crystals **1** (XRD data). Dark blue crystals **2**, shaped as elongated rhombohedra, were selected mechanically. Their quantity was so insignificant that we could study only the crystal structure of **2**. We were unable to find a procedure leading to pronounced amounts of **2**. Note that the first portion of crystals must be quickly filtered off (within 5−15 min after the mixing and cooling). If the reaction mixture is stored for prolonged time, the solid contains only crystals **11** (as in the synthesis of **10** described below). Because of kinetic inertness of crystals **11**, it is possible to quickly settle the mixture of crystals **1** and **2** and separate them from the mother solution within the first few minutes.

$Cu(hfac)_2$L (3, or "Head-to-Head"-1). As in the case of **2**, we were unable to find a procedure leading to pronounced amounts of **3**. The compound formed as an impurity during recrystallization of complex **1** from toluene in the presence of excess L. The crystals of the complex (dark brown rhombohedra) were separated mechanically. After X-ray diffraction analysis of each crystal, the crystals were collected in a quantity sufficient for thermomagnetic measurements.

$Cu(hfac)_2$L (4, or "Head-to-Head"-2). A mixture of $[Cu(hfac)_2]_3L_2 \cdot 2C_6H_6$ (0.1000 g, 0.05 mmol) and L (0.0115 g, 0.05 mmol) was dissolved in CH_2Cl_2 (10 mL), then heptane (10 mL) was added, and the mixture was allowed to stay in an open flask at room temperature. After 2 days, large black rhombohedral crystals formed; they were filtered off, washed with cold heptane, and dried in air. Yield ~80%. The solid consisted of crystals **4** and **1**, among which **4** prevailed. The crystals were separated mechanically.

(25) Ovcharenko, V. I.; Fokin, S. V.; Romanenko, G. V.; Ikorskii, V. N.; Tretyakov, E. V.; Vasilevsky, S. F.; Sagdeev, R. Z. *Mol. Phys.* **2002**, *100*, 1107.

Table 1. Crystallographic Characteristics and Experimental Details

no.	compound	T, K	space group Z	a, Å b, Å c, Å	α, deg β, deg γ, deg	V, Å^3 D_c, g cm^{-3} ΔV, %	I_{hkl} (meas/uniq) R_{int}	R_1 wR_2
	L	293	$P2_1/c$	9.693(2)		1235.5(4)	1889/1765	0.0485
			4	11.438(2)	108.21(3)	1.276	0.0328	0.1342
				11.731(2)				
1	Cu(hfac)$_2$L	293	$P2_1/n$	12.287(2)		2947.8(10)	5449/5191	0.0742
			4	16.181(4)	108.46(1)	1.611	0.0391	0.2106
				15.631(2)				
2	Cu(hfac)$_2$L	293	$P\bar{1}$	12.278(3)	84.86(1)	2939.9(10)	10838/10317	0.0857
			4	15.845(3)	87.11(1)	1.615	0.0480	0.1670
				15.782(3)	74.10(1)			
3	Cu(hfac)$_2$L	293	$P\bar{1}$	10.231(1)	102.93(1)	1469.2(4)	5455/5139	0.0468
			2	11.104(2)	95.17(1)	1.616	0.0168	0.1300
				13.751(2)	102.72(1)			
		173	$P\bar{1}$	10.202(1)	103.00(1)	1418.0(4)	4949/4688	0.0380
			2	10.885(2)	96.03(1)	1.569	0.0174	0.0999
				13.610(2)	102.63(1)			
		123	$P\bar{1}$	10.190(12)	102.56(2)	1390.1(19)	2970/2754	0.0814
			2	10.848(6)	96.54(5)	1.708	0.0533	0.1981
				13.395(6)	102.59(6)	5.4		
4	Cu(hfac)$_2$L	293	$P2_1/n$	10.253(4)		5791(4)	9740/9149	0.0539
			8	37.649(12)	103.23(2)	1.640	0.0393	0.1815
				15.411(6)				
		123	$P2_1/n$	10.189(3)		5549(3)	6619/6618	0.0333
			8	36.981(11)	103.52(2)	1.712	0.0100	0.0833
				15.147(4)		3.7		
5	Cu(hfac)$_2$L·3C$_6$H$_6$	293	$R\bar{3}c$	22.715(3)	90	28687(8)	10541/5590	0.0773
			36	22.715(3)	90	1.521	0.1070	0.1763
				64.199(13)	120			
6	Cu(hfac)$_2$L·6CH$_2$Cl$_2$	293	$R\bar{3}c$	22.581(3)	90	28343(8)	4147/4107	0.0845
			36	22.581(3)	90	1.597	0.1094	0.1981
				64.185(13)	120			
7	Cu(hfac)$_2$L$_2$·1.5C$_7$H$_8$	293	$P2_1/c$	13.056(2)		5120.4(13)	8612/8536	0.0443
			4	22.239(3)	106.58(1)	1.414	0.0293	0.1149
				18.400(3)				
8	[Cu(hfac)$_2$]$_3$L$_2$·2C$_6$H$_6$	293	$P\bar{1}$	12.397(3)	95.69(3)	2169.4(7)	7903/7519	0.0683
			2	13.742(3)	105.77(3)	1.580	0.0271	0.1875
				14.988(3)	114.51(3)			
9	[Cu(hfac)$_2$]3L$_2$·2C$_7$H$_8$	293	$P\bar{1}$	12.383(3)	95.20(3)	2206.3(8)	8097/7707	0.0694
			2	13.824(3)	106.85(3)	1.574	0.0217	0.1941
				15.057(3)	113.14(3)			
10	[Cu(hfac)$_2$]3L$_2$·C$_6$H$_{14}$	293	$P\bar{1}$	13.622(6)	75.02(3)	4228(3)	8255/7815	0.0567
			2	15.000(7)	83.82(4)	1.538	0.0487	0.1667
				21.641(6)	83.20(2)			
11	[Cu(hfac)$_2$]$_3$L$_2$·C$_7$H$_{16}$	293	$P\bar{1}$	12.462(3)	96.90(3)	2123.7(7)	7792/7421	0.0755
			2	13.527(3)	104.20(3)	1.581	0.0146	0.2067
				14.963(3)	115.90(3)			
12	[Cu(hfac)$_2$]$_2$L·0.5C$_6$H$_{14}$	293	$P2_1/n$	13.962(4)	98.66(2)	4817(2)	8793/8430	0.0662
			4	18.806(5)		1.704	0.0183	0.1926
				18.556(5)				

Calculated for $C_{21}H_{19}N_4O_6F_{12}Cu$, %: C, 35.3; H, 2.7; N, 7.8; F, 31.9. Found, %: C, 35.5; H, 2.5; N, 7.7; F, 32.4.

[Cu(hfac)$_2$L]$_6$·3C$_6$H$_6$ (5). A mixture of Cu(hfac)$_2$ (0.1007 g, 0.21 mmol) and L (0.0500 g, 0.21 mmol) was dissolved in benzene (20 mL). The resulting dark brown solution was filtered and slowly concentrated with a flow of air to a volume of ∼10 mL. The resulting blue crystals shaped as hexagonal plates were filtered off, washed with a small amount of cold benzene, and dried in air. Yield 55%. Calculated for $C_{144}H_{132}N_{24}O_{36}F_{72}Cu_6$, %: C, 38.2; H, 2.9; N, 7.4; F, 30.2. Found,: C, 38.7; H, 3.0; N, 7.5; F, 29.8.

[Cu(hfac)$_2$L]$_6$·6CH$_2$Cl$_2$ (6). A mixture of Cu(hfac)$_2$ (0.1007 g, 0.21 mmol) and L (0.0500 g, 0.21 mmol) was dissolved in CH_2Cl_2 (10 mL). To the resulting dark brown solution was added hexane (10 mL), and the mixture was stored in an open flask in a refrigerator. After 2 days, blue crystals shaped as hexagonal plates formed. The substance was filtered off, washed with a small amount of cold hexane, and dried with a flow of air. Yield 45%.

Cu(hfac)$_2$L$_2$·(3/2)C$_7$H$_8$ (7). To a solution of L (0.0500 g, 0.21 mmol) in toluene (3 mL) was added a solution of Cu(hfac)$_2$ (0.0503 g, 0.105 mmol) in toluene (5 mL). The resulting greenish blue solution was filtered and stored at −18 °C for 6 days. The blue crystals were filtered off, washed with a small amount of cold heptane, and dried in air. Yield 60%. Calculated for $C_{32}H_{36}N_8O_8F_{12}Cu$, %: C, 40.4; H, 3.8; F, 23.9. Found, %: C, 40.8; H, 3.9; F, 24.8.

[Cu(hfac)$_2$]$_3$L$_2$·2C$_6$H$_6$ (8). A mixture of Cu(hfac)$_2$ (0.1510 g, 0.32 mmol) and L (0.0500 g, 0.21 mmol) was dissolved in benzene (10 mL). The resulting dark brown solution was filtered and slowly concentrated with a flow of air to a volume of ∼5 mL. The resulting claret red crystals were filtered off, washed with a small amount of cold benzene, and dried in air. Yield 55%. Calculated for $C_{52}H_{40}N_8O_{16}F_{36}Cu_3$, %: C, 33.9; H, 2.2; N, 6.1. Found, %: C, 34.1; H, 2.7; N, 6.1.

[Cu(hfac)$_2$]$_3$·2C$_7$H$_8$ (9). A mixture of Cu(hfac)$_2$ (0.1510 g, 0.32 mmol) and L (0.0500 g, 0.21 mmol) was dissolved in toluene (10 mL). The resulting dark brown solution was filtered and stored at −18 °C overnight. The dark claret red crystals were filtered off, washed with a small amount of cold toluene, and dried in air. Yield 70%. In this procedure, **9** also formed when the initial reagent ratio

was 1:1. Calculated for $C_{66}H_{56}N_8O_{16}F_{36}Cu_3$, %: C, 37.9; H, 2.7; N, 5.4; F, 32.7. Found, %: C, 37.6; H, 2.7; N, 5.7; F, 33.2.

$[Cu(hfac)_2]_3L_2 \cdot C_6H_{14}$ (10). A mixture of $Cu(hfac)_2$ (0.1510 g, 0.32 mmol) and L (0.0500 g, 0.21 mmol) was dissolved with heating to 50 °C in hexane (30 mL). The resulting dark brown solution was filtered and allowed to slowly cool to room temperature. The black prismatic crystals were filtered off, washed with a small amount of cold hexane, and dried in air. Yield 85%. Calculated for $C_{58}H_{54}N_8O_{16}F_{36}Cu_3$, %: C, 34.9; H, 2.7; N, 5.6; F, 34.3. Found, %: C, 34.5; H, 2.8; N, 5.9; F, 35.0.

$[Cu(hfac)_2]_3L_2 \cdot C_7H_{16}$ (11) was synthesized from heptane according to an analogous procedure. Yield (for the initial amount of heptane of 50 mL) 87%. Calculated for $C_{59}H_{56}N_8O_{16}F_{36}Cu_3$, %: C, 35.3; H, 2.8; N, 5.6; F, 34.1. Found, %: C, 34.8; H, 2.8; N, 5.7; F, 34.2.

$[Cu(hfac)_2]_2L \cdot (1/2)C_6H_{14}$ (12). A mixture of $Cu(hfac)_2$ (0.2013 g, 0.42 mmol) and L (0.0500 g, 0.21 mmol) was dissolved with heating to 50 °C in hexane (30 mL). The resulting dark brown solution was filtered and allowed to stay in a refrigerator overnight. The black rhombohedral crystals were filtered off, washed with a small amount of cold hexane, and dried in air. A small amount of fine black crystals **10** was separated from crystals **12** mechanically. Yield 75%. Calculated for $C_{34}H_{28}N_4O_{10}F_{24}Cu_2$, %: C, 33.1; H, 2.3; N, 4.5. Found, %: C, 34.0; H, 2.4; N, 4.7.

X-ray Structure: General Description. All crystals under study are shaped as prisms or elongated rhombohedra. When stored in air, crystals **5**−**12** gradually lose solvent molecules and become turbid. The data were collected on a P4 Bruker AXS automatic diffractometer using the standard procedure (Mo Kα, $\theta/2\theta$ scan mode at a variable rate, $V_{min} = 3$ deg/min, $2.5 < 2\theta < 50°$). The structures were solved by direct methods and refined by full matrix least-squares analysis anisotropically. The hydrogen atoms were partially localized on difference electron density maps and refined isotropically together with non-hydrogen atoms. All calculations and refinements were carried out using SHELX-97 software. Crystal data for the compounds and details of the experiment are listed in Table 1.

Magnetic measurements were carried out on a Quantum Design SQUID magnetometer in the temperature range 2−300 K (magnetic field strength 0.5 T). The paramagnetic susceptibility (χ) was calculated by taking into account the diamagnetic contributions of atoms according to Pascal's scheme. The effective magnetic moment was calculated by the formula $\mu = [(3k/N\beta^2)\chi T]^{1/2} \approx (8\chi T)^{1/2}$, where k is Boltzmann's constant, N is the Avogadro number, and β is the Bohr magneton. The theoretical values of $\mu_{eff}(T)$ for the complexes were calculated in terms of Hamiltonians (1) or (2) for g_{NO} taken to be 2. Exchange interactions between the clusters and the Cu(II) ions not involved in the clusters were taken into account, along with intercluster exchange interactions, by including the nJ' parameter. For Cu(II)−O•−N< exchange clusters, experimental data were processed by using the isotropic spin Hamiltonian:

$$\hat{H} = -2J\hat{s}_{Cu}\hat{s}_{NO} - (g_{Cu}\hat{s}_{Cu} + g_{NO}\hat{s}_{NO})\beta H - 2nJ'\hat{S}\langle\hat{S}\rangle \qquad (1)$$

where s_{Cu} and s_{NO} are the spin values; g_{Cu} and g_{NO} are the g-factors of Cu(II) and >N−•O− group, respectively; $S = s_{Cu} + s_{NO}$ is the total spin of the cluster; J is the exchange parameter of the cluster; nJ' is the intercluster exchange parameter. For the >N−•O−Cu(II)−O•−N< exchange cluster

$$\hat{H} = -2J\hat{s}_{Cu}\hat{s}' - (g_{Cu}\hat{s}_{Cu} + g_{NO}\hat{s}')\beta H - 2nJ'\hat{S}\langle\hat{S}\rangle \qquad (2)$$

where $s' = s_{NO1} + s_{NO2}$ is the total spin of the two radicals, and $S = s_{Cu} + s'$ is the spin of the cluster.[28] Optimal values of spin Hamiltonian parameters are given in Table 4; the corresponding theoretical curves (solid lines) are presented in Figures 4−8.

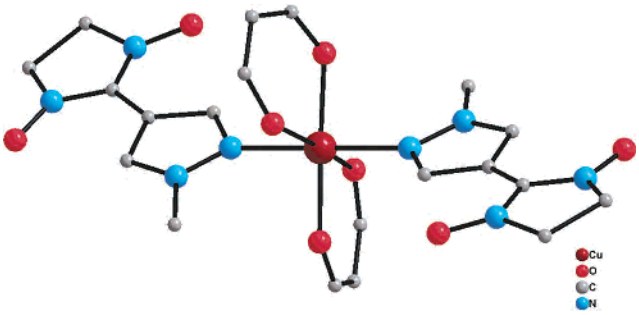

Figure 1. Molecule **7** (hydrogen atoms, geminal methyl groups L, and trifluoromethyl groups of hfac ligands omitted for easy perception).

Results and Discussion

Since the crystal structure was determined for all compounds (**1**−**12**) (Table 1), it is reasonable to begin by discussing the structure of their solid state. For all solid complexes except **7** (Figure 1), the paramagnetic L is a bridging bidentate ligand coordinated via the oxygen atom of one of the N−O groups (O_{NO}) and the unsubstituted nitrogen atom of the pyrazole ring (N_{Pz}). This results in chains with a "head-to-tail" (**1** and **2**) or "head-to-head" (**3** and **4**) motif or in binuclear (**12**), trinuclear (**8**−**11**), and hexanuclear (**5** and **6**) complexes (Figures 2 and 3).

In the binuclear molecule of **12**, each of the two Cu atoms is surrounded by donor atoms forming a square pyramid, where an O_{hfac} atom is at the apex, and the base is formed from the other three O_{hfac} atoms and the O_{NO} atom for Cu(1) or the N_{Pz} atom for Cu(2) (Figure 2a). The Cu(1)−O_{NO} and Cu(2)−N_{Pz} distances are 1.958 and 2.028 Å, respectively. They are close in magnitude to the equatorial Cu−O_{hfac} distances (∼1.95 ± 0.02 Å), but they are much shorter than the Cu−O_{hfac} distances to the apical oxygen atom (∼2.18 ± 0.02 Å) (Table 2).

In trinuclear molecules **8**−**11**, the terminal Cu atoms also have square pyramidal surroundings of five oxygen atoms ($4O_{hfac} + O_{NO}$), with the O_{NO} atom lying at the base of the pyramid at a distance of Cu−O_{NO} < 2 Å (Figure 2b). The central Cu atom has a square bypiramidal environment with O_{hfac} atoms forming an equatorial plane and the two N_{Pz} atoms lying at the apexes of the polyhedron at distances of ∼2.4 Å.

The hexanuclear molecules of **5** and **6** (Figure 2c) may be regarded as molecules formed from six square pyramidal {$Cu(hfac)_2L$} molecules with equatorial coordination of L via the N_{Pz} atom (Cu−N_{Pz} distances equal 2.022 and 2.062 Å in **5** and **6**, respectively) and cis coordination of the two hfac anions. This structural fragment is also present in the above-described binuclear molecules **12**. Under the con-

(26) Shklyaev, A. A.; Anufrienko, V. F. *Zh. Strukt. Khim.* **1975**, *16*, 1082 (Russ. Ed.).
(27) Sagdeev, R. Z.; Voronov, V. K.; Podoplelov, A. V.; Ushakov, I. A.; Chemezov, A. N.; Fursova, E. Y.; Fokin, S. V.; Romanenko, G. V.; Reznikov, V. A.; Ovcharenko, V. I. *Russ. Chem. Bull.* **2001**, 2078.
(28) Ovcharenko, I. V.; Shvedenkov, Yu. G.; Musin, R. N.; Ikorskii, V. N. *J. Struct. Chem.* **1999**, *40*, 29.

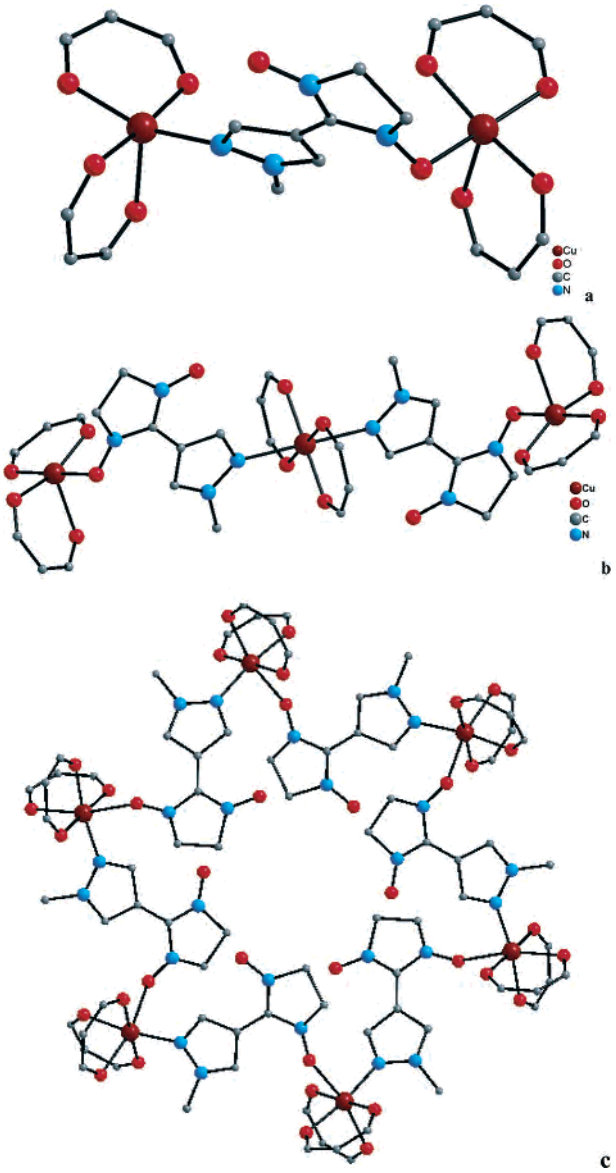

Figure 2. Structure of binuclear molecule **12** (a), trinuclear molecules **8**−**11** (b), and hexanuclear molecules **5** and **6** (c) (hydrogen atoms, geminal methyl groups L, and trifluoromethyl groups of hfac ligands omitted for easy perception).

densation of six {Cu(hfac)$_2$L} molecules into the hexanuclear ring, the square pyramidal environment of Cu in {Cu(hfac)$_2$L} is completed to square bipyramidal with cis-coordinated paramagnetic ligands. The axial positions in the square bipyramid are occupied by the O_{NO} atoms (∼2.46 ± 0.02 Å) and one of the O_{hfac} atoms (2.20 ± 0.01 Å). Note that, in both structures **5** and **6**, the molecules of the complex are arranged in layers with solvent (C_6H_6 or CH_2Cl_2) molecules lying between them.

In solid **7**, the N−O groups are not coordinated. The N−O bond lengths are therefore the same (1.267−1.282 Å) within the error of experiment and almost the same as those in free L (1.281 and 1.283 Å). In **8**−**12**, coordination of one of N−O groups into the equatorial plane, forming short (<2 Å) Cu−O_{NO} bonds, causes lengthening of the N−O bond by 0.02−0.03 Å in the coordinated fragment and nearly the same shortening of the N−O bond is observed in the noncoordinated fragment (Table 2). In hexanuclear molecules **5** and **6**, coordination of O_{NO} atoms to the axial positions with long Cu−O_{NO} distances does not change the N−O bond lengths in the paramagnetic ligand.

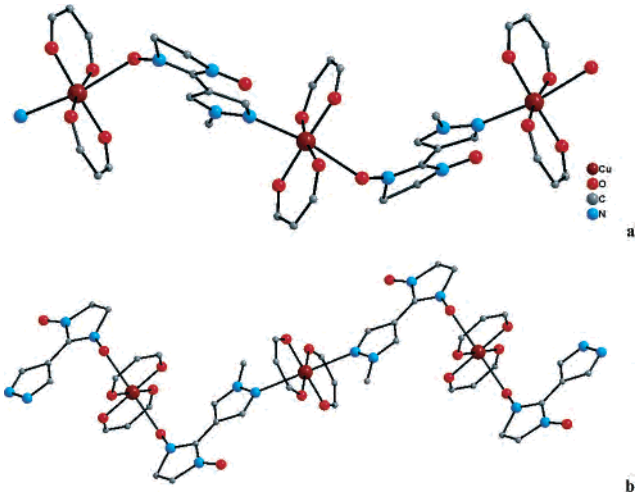

Figure 3. Structure of chains with a "head-to-tail" motif in **1** and **2** (a) and "head-to-head" motif in **3** and **4** (b) (hydrogen atoms, geminal methyl groups L, and trifluoromethyl groups of hfac ligands omitted for easy perception).

In the solid, **1** is constructed from zigzag chains with a "head-to-tail" motif (Figure 3a). The Cu atom is surrounded in the equatorial plane by four O_{hfac} atoms of the two hfac anions (Cu−O_{hfac} = 1.936−1.962 Å). The O_{NO} and N_{Pz} atoms occupy the axial positions at distances of 2.484 and 2.329 Å, respectively. The N−O distances in L are nearly the same (1.288 Å) because the Cu−O distance to the nitroxyl oxygen is long enough. The shortest distances between the noncoordinated O_{NO} atoms of neighboring chains are at least 4.104 Å, and F···F distances are 2.922 Å. In compound **2**, the chains have a similar structure. However, because of the presence of two different CuO_5N coordination units, the symmetry is lowered, and the crystallographically unique part of the structure is doubled (Table 3). In the structure of **2**, the CuON angles at the coordinated O_{NO} atom in the alternating CuO_5N units differ (130.0° and 149.9°), whereas in **1** they are the same (139.4°).

The zigzag chains with a "head-to-head" motif in **3** and **4** involve two crystallographically independent Cu atoms; the environment of the central atom is centrosymmetric in **3** and acentric in **4**. The axial positions are occupied by the O_{NO} atoms at one Cu atom and by the N_{Pz} atoms of the two L's at the other (Figure 3b). In contrast to **1** and **2**, the Cu−N_{Pz} distances are longer than Cu−O_{NO} (Table 3). The fundamental difference between the structures of **3** and **4** lies in the magnitude of the Cu−O_{NO} distances in **4** (2.395 and 2.459 Å) and CuON angles in **4** (131.3° and 140.6°), which is not observed in **3**. The shortest interchain distances in **3** are 3.906 Å (O_{NO}···O_{NO}) and 3.047 Å (F···F). In **4**, the analogous values are 3.917 and 3.008 Å, respectively.

Thus, quite a few phases may be obtained in a Cu(hfac)$_2$−L system depending on the reagent ratio, solvent, and crystallization conditions. Unfortunately, phase diagrams cannot be constructed in this case, since the

Table 2. Selected Bond Lengths (Å) and Bond Angles (deg) for Compounds **5**−**12**

	5	**6**	**7**	**8**		**9**		**10**		**11**		**12**	
	$[Cu(hfac)_2L]_6$· $3C_6H_6$	$[Cu(hfac)_2L]_6$· $6CH_2Cl_2$	$Cu(hfac)_2L_2$· $1.5C_7H_8$	$[Cu(hfac)_2]_3L_2$· $2C_6H_6$		$[Cu(hfac)_2]_3L_2$· $2C_7H_8$		$Cu(hfac)_2]_3L_2$· C_6H_{14}		$[Cu(hfac)_2]_3L_2$· C_7H_{16}		$[Cu(hfac)_2]_2L$· $0.5C_6H_{14}$	
T, K	293	293	293	293	293	293	293	293	293	293	293	293	293
coord core	*uuc*-CuO_5N	*uuc*-CuO_5N	CuO_4N_2	CuO_5	CuO_4N_2	CuO_5	CuO_4N_2	CuO_5	CuO_4N_2	CuO_5	CuO_4N_2	CuO_5	CuO_4N
Cu−O_L	2.481(6)	2.444(4)		1.934(4)		1.936(4)		1.980(4) 1.924(4)		1.932(1)		1.958(3)	
Cu−N_{Pz}	2.022(7)	2.062(4)	2.033(5) 2.045(5)		2.392(4)		2.402(4)		2.411(2)		2.411(5) 2.430(5)		2.028(5)
Cu−O_{hfac}	1.982(6) 1.920(6) 1.932(6) 2.217(6)	1.830(4) 1.988(3) 1.906(4) 2.193(3)	2.217(5) 2.004(5) 1.999(4) 2.294(5)	1.957(3) 2.178(5) 1.951(4) 1.915(4)	1.954(3) 1.962(3)	2.175(5) 1.942(4) 1.913(4) 1.963(4)	1.957(3) 1.959(4)	1.958(4) 2.181(4) 1.968(4) 1.935(4) 2.191(4) 1.989(4) 1.925(4) 1.975(4)	1.963(1) 1.950(1)	2.177(2) 1.958(1) 1.904(1) 1.952(1)	1.958(4) 1.956(4) 1.978(3) 1.926(4)	1.923(4) 1.957(4) 2.197(4) 1.943(4)	1.947(4) 2.174(5) 1.967(4) 1.934(4)
N−O(−Cu)	1.273(8)	1.275(5)		1.298(6)		1.308(6)		1.306(6) 1.305(5)		1.301(2)		1.307(5)	
N−O	1.277(8)	1.254(6)	1.267(6) 1.272(6) 1.274(6) 1.282(6)	1.261(6)		1.275(7)		1.272(7) 1.275(6)		1.265(2)		1.248(6)	
∠CuON	148.5(5)	152.3(3)		120.3(3)		119.7(3)		120.7(3) 118.3(3)		119.5(1)		118.8(3)	
∠Pz−CN_2	5.0(8)	7.7(7)	2.9(4) 4.4(6)	1.9(7)		2.8(7)		2.0(2) 3.2(2)		2.0(2)		11.8(8)	

Table 3. Selected Bond Lengths (Å) and Bond Angles (deg) for Compounds **1**−**4**

	1	**2**	**3**						**4**			
	$Cu(hfac)_2L$	$Cu(hfac)_2L$	$Cu(hfac)_2L$						$Cu(hfac)_2L$			
T, K	293	293	293	293	173	173	123	123	293	293	123	123
coord core	CuO_5N	CuO_5N	CuO_6	CuO_4N_2	CuO_6	CuO_4N_2	CuO_6	CuO_4N_2	CuO_6	CuO_4N_2	CuO_6	CuO_4N_2
Cu−O_L	2.484(5)	2.507(7) 2.507(6)	2.339(3)		2.295(2)		2.174(7)		2.395(3) 2.459(3)		2.356(2) 2.447(2)	
Cu−N_{Pz}	2.329(5)	2.323(7) 2.298(7)		2.557(3)		2.496(2)		2.473(8)		2.543(3) 2.541(3)		2.482(3) 2.441(3)
Cu−O_{hfac}	1.936(4) 1.950(4) 1.956(4) 1.962(4)	1.946(6) 1.964(6) 1.930(6) 1.942(6) 1.937(6) 1.947(6) 1.968(6) 1.959(7)	1.957(3) 1.969(2)	1.943(2) 1.959(2)	1.953(2) 1.995(2)	1.948(2) 1.970(2)	1.926(9) 2.132(8)	1.936(7) 1.970(6)	1.957(3) 1.952(3) 1.965(3) 1.934(3)	1.969(3) 1.961(3) 1.966(3) 1.951(3)	1.952(2) 1.952(2) 1.963(2) 1.940(2)	1.980(2) 1.961(2) 1.976(2) 1.960(2)
N−O(−Cu)	1.288(6)	1.294(8) 1.283(8)	1.288(4)		1.294(3)		1.300(11)		1.284(4)	1.293(4)	1.294(3)	1.291(3)
N−O	1.287(8)	1.267(8) 1.279(8)	1.273(3)		1.279(3)		1.294(9)		1.275(4)	1.276(4)	1.284(3)	1.279(4)
∠CuON	139.4(4)	130.0(5) 149.9(6)	132.1(2)		129.8(2)		128.6(6)		131.3(2) 140.6(3)		129.1(2) 139.8(2)	
∠Pz−CN_2	13.3(6)	7.8(5) 8.6(6)	5.6(4)		6.8(3)		7.9(10)		7.0(4)	0.9(6)	8.5(4)	2.7(4)

complexes are not stable enough when stored in solution for a long time. Some of them had to be filtered off immediately after crystallization, because prolonged storage in solution led to another compound (e.g., **2**). Moreover, crystals **1** and **3**−**12** grew in the course of gradual evaporation of the solvent or a mixture of solvents. Crystals **1**, **2**, **10**, and **11** grew when the temperature of the mother liquor was lowered from 50 to 20 °C. As a matter of fact, crystals **1**−**12** were grown in nonequilibrium conditions, which is generally typical for synthetic procedures of metal complexes with nitroxides. Variation of many parameters during syntheses of **1**−**12** hinders the perception of a synthetic system as an entity. On the basis of synthetic and structural data, however, one can conjecture the following.

Scheme 1

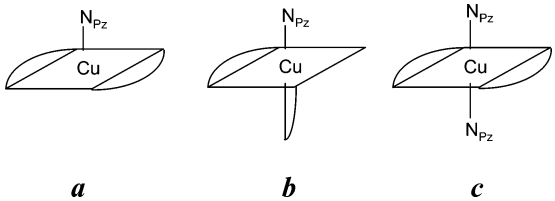

a ***b*** ***c***

Synthesis of **7**−**12**, i.e., phases with $Cu(hfac)_2/L = 1:2$, 3:2, and 2:1, mainly depends on the initial reagent ratio. As is known, when the ratio of $Cu(hfac)_2$ to N-containing ligand is 1:1, the solution mainly has molecular forms with coplanar (Scheme 1, **a**) and noncoplanar (Scheme 1, **b**) arrangements of hfac anions, whose ratio depends on temperature.[26] For

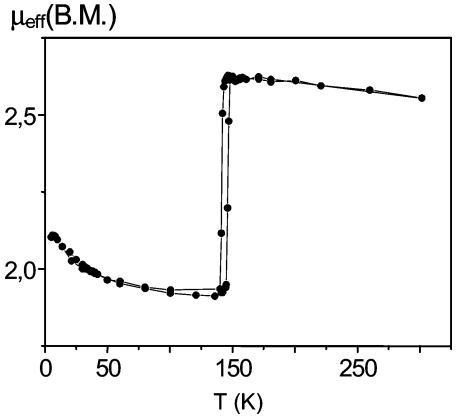

Figure 4. Dependence of $\mu_{eff}(T)$ for **1**.

Table 4. Schemes of Exchange Clusters (in Brackets) and Optimal Parameters g_{Cu}, J, and $J'z$

complex	exchange cluster	g_{Cu}	J, K	$J'z$, K
1 (T < 150 K)	[Cu−O−N<]···Cu	2.34	10.5	0.23
1 (T > 150 K)	[Cu−O−N<]···Cu	2.11	26.8	−0.9
4	[>N−O−Cu−O−N<]···Cu	2.10	19.6	−1.3
5	[Cu−O−N<]···Cu	2.03	19.2	−1.5
7	[>O−N−Cu−N−O<]	2.14	−1.7	−0.9
8	[Cu−O−N<]···Cu···[>N−O−Cu]	2.33	−647	−0.5
9	[Cu−O−N<]···Cu···[>N−O−Cu]	2.33	−526	−0.15
10	[Cu−O−N<]···Cu···[>N−O−Cu]	2.30	−686	−0.44
11	[Cu−O−N<]···Cu···[>N−O−Cu]	2.40	−396	−1.36
12	[Cu−O−N<]···Cu	2.24	−570	−0.27

mixed-ligand complexes of Cu(hfac)$_2$ with N-donor ligands, the fraction of form **b** is higher at reduced temperatures.[26] The presence of a large amount of L in the reaction mixture certainly shifts the equilibrium toward form **c** (Scheme 1), which favors the growth of crystals **7** (and formation of chains **3** and **4** with a "head-to-head" motif discussed below). Therefore, **7** was isolated when the reagent ratio in the system was L/Cu(hfac)2 > 2.

Clearly, when Cu(hfac)$_2$/L > 1, the equilibrium is also shifted toward form **c**. The fraction of form **c** increases further with the amount of Cu(hfac)$_2$ in solution; at the same time, reaching Cu(hfac)$_2$/L = 3:2 creates favorable conditions for the formation of compounds **8**−**11**. The trinuclear molecules of **8**−**11** may be regarded as some kind of fragments **c** completed by the Cu(hfac)$_2$ matrixes at the O_{NO} atoms. Note that treatment of a solution of **7** with a double quantity of Cu(hfac)$_2$ easily converts **7** into **9** and may be employed as a method for the preparation of **9**. Solids **8**−**11** are formed by similar trinuclear fragments; they differ in solvation molecules alone depending on the solvent from which the compound crystallized.

When the ratio Cu(hfac)$_2$/L increased to 2:1, conditions proved to be favorable for synthesis of binuclear compound **12**. A transition from trinuclear (**8**−**11**) to binuclear (**12**) fragments may result from cleavage of long Cu−N bonds (∼2.4 Å) in trinuclear molecules **8**−**11** and formation of much more stable Cu−O and Cu−N (∼2 Å) bonds in binuclear molecules **12**. It is equally important that **12** was isolated under conditions of cooling of the reaction mixture, favoring the formation of the conformation **b** (Scheme 1, Figure 1a) with noncoplanar hfac anions. Also, note that at room temperature **12** has a slightly better solubility than

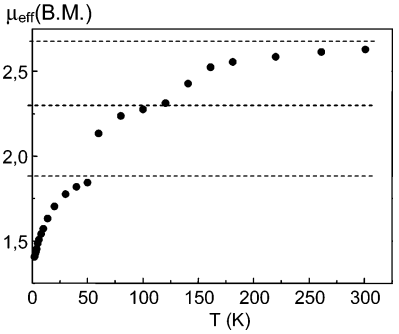

Figure 5. Dependence of $\mu_{eff}(T)$ for **3**.

Scheme 2

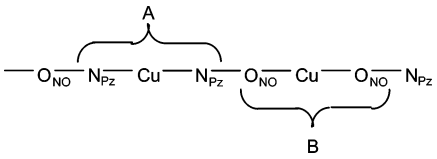

trinuclear complexes (at 295 K, solubility in hexane is 9.8 × 10^{-4} M for **12**, 3.6 × 10^{-4} M for **8**, and 3.3 × 10^{-4} M for **10**). The lower solubility of complexes with Cu(hfac)$_2$/L = 3:2 led to the formation of minor amounts of impurity crystals **10** (to crystals **12**), which were separated mechanically (see Experimental Section, synthesis of **12**). Treatment of **12** with an additional amount of L in any solvent readily converted **12** into trinuclear **8**−**11**. Similarly, addition of Cu(hfac)$_2$ to Cu(hfac)$_2$/L = 3:2 to a (hexane, heptane, toluene, or benzene) solution at room temperature always led to dissolution of **1** and further crystallization of **8**−**11** since **1** also has a slightly higher solubility (5.0 × 10^{-4} M at 295 K) in hexane than trinuclear complexes **8**−**11**.

Chain polymer complex **1** immediately forms as a solid when a hexane or heptane solution is cooled from 50 °C to room temperature provided that Cu(hfac)$_2$/L = 1:1 (i.e., mononuclear species with conformation **a** prevail, Scheme 1). It is plain that conformation **a** favors the construction of a polymer with a "head-to-tail" motif. Its polymorphs **2** and **3** are metastable phases, uncontrollably and unreproducibly formed as impurities in the form of a few crystals in **1**, which are separated mechanically. The procedure giving modification **4** with a "head-to-head" chain polymer motif is reproducible. To synthesize **4**, as a substrate we used trinuclear complex **8** containing some kind of molecular template for the construction of polymer chains with a "head-to-head" motif. Crystallization of **4**, however, always produced a substantial amount of **1** (up to ∼1/3). Therefore, crystals **4** and **1** also always had to be separated mechanically (see Experimental Section, synthesis of **4**).

It should rather be deemed a success that complex **1**, possessing unusual magnetic properties, is readily accessible in a Cu(hfac)$_2$−L synthetic system. It can be prepared not only by the above-described procedures, but also from warm hexane or heptane solutions of **7**−**12** with additions of Cu(hfac)$_2$ or L to Cu(hfac)$_2$/L = 1:1. On the other hand, complex **3**, whose magnetic properties also deserve special investigation, could be isolated with great difficulty, if at all, although the conditions leading to synthesis of **3** and **4**

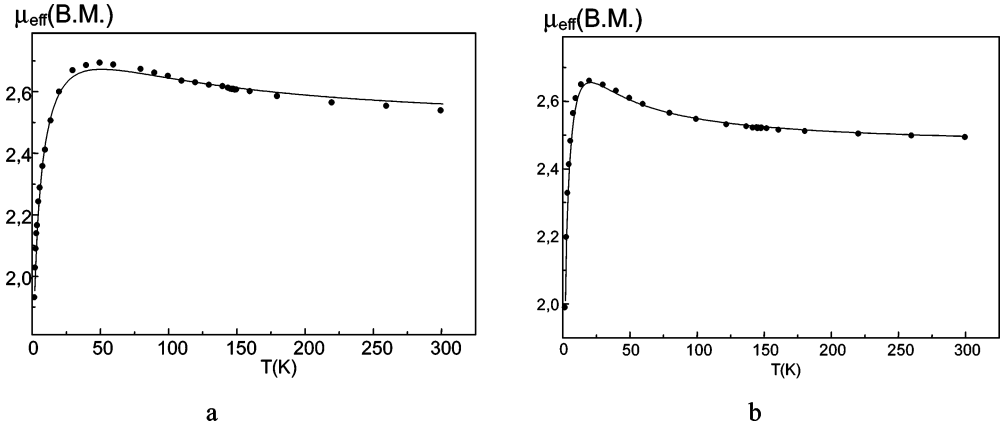

Figure 6. Dependence of $\mu_{eff}(T)$ for **4** (a) and **5** (b).

with a "head-to-head" motif may well be rationalized. Complex **4** was obtained by treatment of **8** with an equivalent amount of L; i.e., as noted above, the symmetric $[Cu(hfac)_2]_3L_2$ fragments served as convenient molecular templates for the construction of polymer chains with a "head-to-head" motif. In a similar way, impurity crystals **3** were formed by recrystallization of **1** from toluene in the presence of excess L. The presence of excess L apparently leads to an increased fraction of form **c** (Scheme 1) in solution, which is favorable for the formation of a chain with a "head-to-head" motif.

Formation of the hexanuclear polymorphic modifications of $Cu(hfac)_2L$ (**5** and **6**) is much easier to understand. Assembly of hexanuclear molecules requires that the solution contains mononuclear molecules with a **b** conformation (Scheme 1). Of all the solvents used, benzene always promoted the formation of this conformation, readily giving crystals **5** irrespective of crystallization conditions (reagent ratio 1:1). To obtain compound **6** with a similar hexanuclear structure (Figure 2c), product crystallization was fulfilled at a low temperature. As is known, at reduced temperature, the stereochemically nonrigid mononuclear metal-containing matrixes tend to go from conformation **a** to conformation **b**.[26,27]

At reduced temperatures, solid **1** undergoes a structural phase transition, which entails a magnetic effect similar to spin crossover in the character of the $\mu_{eff}(T)$ dependence (Figure 4). The origin of this effect was explained elsewhere.[24] It was shown that the abrupt transition at 141 K (cooling) or 146 K (heating) on the $\mu_{eff}(T)$ curve is caused by a rearrangement of the CuO_5N Jahn−Teller coordination polyhedra. In half these polyhedra, the $Cu-O_{NO}$ bond is drastically shortened (from 2.35−2.45 to 2.0 Å). This leads to a change from weak ferromagnetic to strong antiferromagnetic interaction in $Cu-O^{\bullet-}N<$ exchange clusters and hence to a decrease in μ_{eff} by a factor of $\sqrt{2}$. Table 4 lists the values of the exchange parameters before and after the transition.

The magnetic properties of **3** deserve special attention. The $\mu_{eff}(T)$ dependence for **3** is a three-step curve (Figure 5). In Figure 5, the steps are denoted by equidistant dotted lines. The values of μ_{eff} corresponding to the dotted lines are easily understandable if we assume the following structural dynamics of $>N-\bullet O-Cu-O\bullet-N<$ exchange clusters. At first, a phase transition takes place at ~135 K, which is accompanied by a dramatic shortening of $Cu-O_{NO}$ distances in half of all CuO_6 coordination units containing the $>N-\bullet O-Cu-O^{\bullet-}N<$ exchange clusters (denoted by **B** in Scheme 2), lowering the total spin of the exchange cluster to 1/2. On cooling to ~60 K, the second phase transition takes place, decreasing the total spin in the rest of exchange clusters **B** to 1/2. If we take that $g_{Cu} = 2$ and neglect the exchange effects, μ_{eff} must be 2.45 μ_B for **3** at high temperatures. The value of μ_{eff} must decrease to 2.12 μ_B after the total spin has diminished in half of all **B** units, as described above, and to 1.73 μ_B after the total spin has diminished in the other half. In Figure 5, the dotted lines correspond to these values augmented by ~0.2 μ_B. (The real value of g_{Cu} is at least 2.2.)

Note that even at room temperature the $Cu-O_{NO}$ distances in exchange clusters **B** of **3** are noticeably shorter (2.339 Å) than those in **1**, **2**, or **4** (Table 3). A low-temperature X-ray diffraction experiment for **3** has established that at $T = 173$ K and lower (to 123 K) the $Cu-O_{NO}$ bonds in the solid are shortened to 2.174 Å and the O_{NO} atom is gradually shifted from axial to equatorial position (Table 3). Simultaneously, two $Cu-O_{hfac}$ distances in CuO_6 coordination units are lengthened (Table 3). As is known, in the case of equatorial coordination, the characteristic $Cu-O_{NO}$ bond length is ~2.0 Å.[29] Therefore, structure refinement with an averaged value of $Cu-O_{NO} = 2.174$ Å, but not with two groups of bond lengths ($d = 2.0$ Å in one and 2.34 Å in the other) after the first transition (i.e., at $T = 123$ K), indicates that half of all $>N-\bullet O-Cu-O^{\bullet-}N<$ exchange clusters with drastically shortened $Cu-O_{NO}$ bond lengths are distributed over crystal **3** randomly. Notably, in **A** units (Scheme 2) in the temperature range from 293 to 123 K, the observed shortening of the axial $Cu-N_{Pz}$ bond lengths is much smaller (Table 3). Unfortunately, we were unable to perform an X-ray diffraction investigation of **3** below 60 K. However, it is evident that below 60 K all $Cu-O_{NO}$ bonds in all CuO_6 units must be shortened to ~2 Å and that a lengthened $O_{hfac}-Cu-O_{hfac}$ axis must be formed in CuO_6 Jahn−Teller units, as observed elsewhere.[24,25] It is also useful to compare the changes in

(29) Orpen, A. G.; Brammer, L.; Allen, F. H.; Kennard, O.; Watson, D. G.; Taylor, R. *J. Chem. Soc., Dalton Trans.* **1989**, S1−S83.

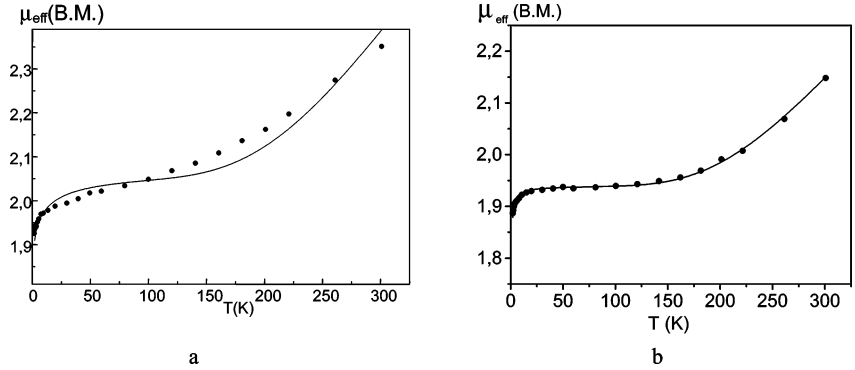

Figure 7. Dependence of $\mu_{eff}(T)$ for **9** (a) and **12** (b).

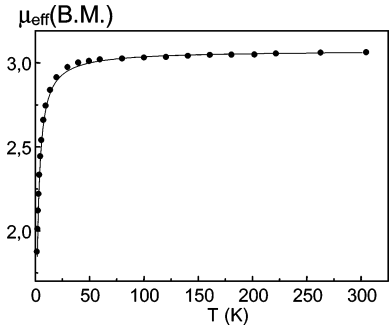

Figure 8. Dependence of $\mu_{eff}(T)$ for **7**.

the Cu−O_{NO} and Cu−N_{Pz} bond lengths due to the cooling of crystals **3** and their structural analogues **4** (Table 3). The Cu−N_{Pz} bonds in **3** and **4** are shortened by the same value, whereas for the Cu−O_{NO} bonds the shortening in **3** is appreciably greater compared to that in **4**. On cooling, the O_{NO} atoms in the CuO_6 coordination units of **4** remain in the axial positions. Therefore, the $\mu_{eff}(T)$ curve for **4** does not exhibit any anomalies (Figure 6). Note that the asymptotic values of μ_{eff} in the region of thermally induced spin transitions in **1** and **3** are close (∼2 and 2.6 μ_B, cf. Figures 4 and 5), since around 50 K in both **1** and **3** the contribution of half of all spins to magnetic susceptibility disappears. The vanishing occurs within one step in **1** and two steps in **3**.

For **4**−**12**, no magnetic effects similar to those discussed above have been recorded. For **4**, as well as for hexamer complexes **5** and **6** with O_{NO} atoms lying in the axial positions of the octahedron, exchange interactions between the odd electrons of Cu(II) and nitroxyl fragments are ferromagnetic. On the $\mu_{eff}(T)$ curves, this shows itself as an increased effective magnetic moment at reduced temperatures (Figure 6). Figure 6b shows the $\mu_{eff}(T)$ curve for only one hexanuclear complex (**5**) because for the other (**6**) the curve is similar. The values of exchange parameters for **5** are listed in Table 4.

For **8**−**12**, where the O_{NO} atoms occupy one of the positions at the base of the square pyramid in the CuO_5 unit, the exchange interactions are antiferromagnetic, as reflected in the decreased effective magnetic moment at reduced temperatures. Figure 7a shows the typical $\mu_{eff}(T)$ curve for trinuclear complexes. Due to the sufficiently strong antiferromagnetic exchange interactions between the odd electrons of the Cu(II) ion and those of the equatorially coordinated nitroxide, μ_{eff} of **8**−**12** tends toward the value of ∼1.9 μ_B at low temperatures, which is due to only Cu^{2+} ions in CuO_4N_2 (**8**−**11**) or CuO_4N (**12**) units. In solid **7**, where the paramagnetic centers are far from one another, the value of μ_{eff} does not change when the sample is cooled to 50 K and remains ∼3.1 μ_B, which corresponds to the contribution from three weakly coupled spins. This is the consequence of the fact that indirect exchange via the heterocycle is less effective than direct exchange.

Conclusions

Thus, investigation of the products of $Cu(hfac)_2$ interaction with spin-labeled pyrazole has revealed a whole family of heterospin compounds **1**−**12** differing in the composition and/or structure of the solids. These compounds often crystallized as mixtures of products. The mixtures, however, could be separated mechanically (with further X-ray diffraction analysis of the crystals) because the solids formed as reasonably perfect crystals. When the crystals of the separated complexes were practically identical in color and shape, each crystal of the sample was analyzed by X-ray diffraction before magnetic measurements. It was found that even seemingly insignificant changes in the structure of the solid heterospin complex can substantially modify the magnetic properties of the compound. Therefore, in this paper, we emphasize that the stereochemically nonrigid $Cu(hfac)_2$ matrix, widely used in heterospin system design, conceals tremendous ambiguity with respect to structures and compositions of products with polyfunctional nitroxides. However, not all products will potentially have nontrivial magnetic properties.

Acknowledgment. This work was supported by RFBR (Grants 03-03-32518, 02-03-33112), BRHE (Grants NO-008-X1, Y1-C-08-03, 3H-269-03), Minobr (E02-5.0-188) and the "Integration" Program.

Supporting Information Available: Crystallographic data in CIF format. This material is available free of charge via the Internet at http://pubs.acs.org.

IC034964D